UNIVERSITY OF BIRMINGHAM

Evolutionary computing to determine the skin friction capacity of piles embedded in clay and evaluation of the available analytical methods

Alzabeebee, Saif; Chapman, David

[Link to publication on Research at Birmingham portal](#)

Evolutionary computing to determine the skin friction capacity of piles embedded in clay and evaluation of the available analytical methods

Saif Alzabeebee, BSc (Hons), MSc (Hons), PhD, GMICE

Geotechnical Engineer, Amey Consulting, International Design hub, The Colmore Building, Birmingham, United Kingdom, B4 6AT

E-mail: Saif.Alzabeebee@gmail.com; Saif.Alzabeebee@amey.co.uk

David N. Chapman, BSc (Hons), DIS, PhD, CEng, MICE, FHEA

Professor of Geotechnical and Underground Engineering, School of Engineering, University of Birmingham, Edgbaston, Birmingham, United Kingdom, B15 2TT

E-mail: D.N.Chapman@bham.ac.uk

Abstract

Deep foundations are very important elements in the routine design of railways and bridges when the loads applied due to these important structures are higher than the bearing capacity of the soil. However, the methods currently available to calculate the bearing capacity of driven piles embedded in clay have been developed based on empirical factors derived from limited tests. Hence, further assessment of these methods and the development of new methods are urgently required. This paper discusses the development of a new robust model to calculate the skin friction capacity of driven piles using the multi-objective evolutionary polynomial regression (MOGA-EPR) analysis. The paper also evaluates the accuracy of the available analytical methods. Real field results of skin friction capacity of driven piles have been used to achieve the objectives of the study. The results showed that the MOGA-EPR predicts the skin friction of driven piles with an excellent accuracy and better than the available analytical methods, with a mean absolute error (MAE), a root mean square error ($RMSE$), mean (μ), a standard deviation (σ), a coefficient of determination (R^2), the variance account for (VAF) and $a20 - index$ of 3.4, 4.6, 1.03, 0.24, 0.98, 99, and 0.75, respectively, for the training data, and 4.2, 5.3, 1.12, 0.15, 0.91, 97 and 0.77, respectively, for testing data. In addition, a novel model to predict the skin friction capacity of driven piles has been proposed based on the MOGA-EPR analysis and this model can be used by engineers and researcher with confidence. The evaluation of the analytical methods illustrated that the Lambda method accuracy is better than the Alpha and Beta methods as this method scored a less mean error (MAE = 7.8 and $RMSE$ = 12.5), a less standard deviation (σ = 0.21), a higher coefficient of determination (R^2 = 0.91), higher value for the variance account for (VAF=89) compared with the other analytical methods. In addition, the Beta method scored lowest compared with the other analytical methods with MAE, $RMSE$, μ, σ, R^2, VAF and $a20 - index$ of 17.2, 28.0, 1.07, 1.00, 0.55, 40 and 0.37, respectively. The findings of this study will help to achieve robust calculations of pile capacity and reduce uncertainty associated with the choice of the analytical method used in the design of driven piles in clay.

Highlights:

54

55   - A novel mathematical model has been proposed to predict the skin friction
56   capacity of driven piles embedded in clay.
57   - The Lambda method produced the lowest error and highest coefficient of
58   determination compared with the other analytical methods.
59   - The Beta method scored lowest in the assessment of the current analytical
60   methods.

61

62

63

64

65

66

67

68

69

70

71

72

73

74

1. Introduction

Deep foundations are very important elements in the design of offshore structures, high-rise buildings, railways and bridges when the loads applied due to these important structures are higher than the bearing capacity of the soil (Li et al., 2019). The urgent demand for the expansion of such heavy structures has been the main reason for more reliable and robust design methods to accurately predict the bearing capacity of deep foundations as this is the main factor controlling the design of deep foundations (Doherty and Gavin, 2011; Alkroosh et al., 2015). The main issue is that the design methods used to predict the bearing capacity of deep foundations have been developed based on factors derived from limited tests (Doherty and Gavin, 2011). Therefore, the accuracy of these design methods requires further assessment and testing. In addition, and due to the complexity of the pile behaviour and the limited tests used to develop the design methods, many previous studies have attempted to use data driven methods to predict the bearing capacity and settlement of deep foundations (Singh and Walia, 2017; Shahin, 2016). These previous studies are summarized in Table 1, the summary includes the data driven method/s each study considered, the input parameters, the output of the data driven method/s and the number of data points used.

In addition to Table 1, there are several studies that have been conducted on the skin friction capacity of piles due to the importance of skin friction in practice as most of the piles are designed to allow very small settlement. The acceptance of a very small settlement in practice means that the routine design of these piles is based on the skin friction, as the end bearing capacity requires a settlement equal to or more than 10% of the diameter of the pile and such settlement is not acceptable in practice. Most of the past studies on the skin friction capacity have focused on the use of data driven methods to predict pile capacity, while there is very limited work concerned with the evaluation of the accuracy of the current analytical methods.

Goh (1995) used artificial neural networks (ANN) to predict the skin friction capacity of driven piles embedded in clay and found that the ANN achieved good prediction of the skin friction, where the coefficient of correlation (R) ranged between 0.86 to 0.99 for the training data (the data used in the development of the ANN model) and 0.94 to 0.96 for the testing data. Goh (1995) also found that ANN predicted the skin friction

4

107 capacity with an accuracy better than the Alpha and Beta methods (Alpha and Beta
108 methods are analytical methods developed to predict the skin friction capacity of pile
109 embedded in cohesive soils and will be discussed in the next section), where the R for
110 the Alpha and Beta methods was equal to 0.98 and 0.73 for the training data, and 0.89
111 and 0.70 for the testing data. Cherubini and Vessia (2007) evaluated the accuracy of
112 the Alpha method in predicting the skin friction capacity of bored piles embedded in
113 clay.

114 Samui (2008, 2011) and Prayogo (2018) used a support vector machine (SVM)
115 approach to predict the skin friction capacity of piles embedded in clay and also found
116 that SVM provided good prediction of the skin friction capacity as the SVM produced
117 low root mean square error values (which ranged between 4.4 to 13.9), low mean
118 absolute error values (which ranged between 3.2 to 9.4), and high R values (which
119 ranged between 0.93 to 0.99). Suman et al. (2016) tested the capabilities of
120 multivariate adaptive regression splines (MARS) and functional networks (FN) to
121 predict the skin friction of driven piles embedded in clay. Suman et al. (2016) found
122 that these methods predicted the skin friction capacity with an accuracy better than
123 the ANN, SVM, Alpha and Beta methods, as these methods scored lower mean
124 absolute error values and lower root mean square error values.

125 Moayedi and Hayati (2018b) developed design charts and a mathematical model to
126 predict the skin friction capacity of driven piles embedded in clay. The design chart
127 was developed based on ANN and the mathematical model was developed based on
128 genetic programing (GP). Samui (2019) used Gaussian Process Regression (GPR)
129 and Minimax Probability Machine Regression (MPMR) to predict the skin friction of
130 driven piles embedded in clay and found that these methods estimated the skin friction
131 capacity better than the ANN. The calculated mean absolute error was equal to 3.2,
132 2.0 and 2.0 for the ANN, GPR and MPMR, respectively. In addition, the calculated
133 mean root square error for the aforementioned methods was equal to 5.3, 4 and 4,
134 respectively.

135 Based on the literature review it is clear that many attempts have been made to predict
136 the skin friction capacity of piles embedded in clay using data driven techniques, i.e.
137 using ANN, SVM, MARS, FN, GP, GPR and MPMR. However, ANN is a black box
138 method as it does not give the relationship between the dependent and the

independent variables (Faramarzi, 2011); hence, such a technique does not clearly show the influence of the pile length, pile diameter, undrained shear strength and effective stress on the skin friction capacity. Furthermore, SVM, MARS, FN, GP, GPR and MPMR provide complicated models, which cannot be easily interpreted and used. Also, no study in the literature has evaluated the capabilities of multi-objective evolutionary polynomial regression analysis (MOGA-EPR) in predicting the skin friction capacity of piles, although this method provides robust and simple mathematical models as demonstrated in many studies in the literature (Ahangar-Asr et al., 2014, 2016, 2018; Fiore et al., 2016; Alzabeebee et al., 2018, 2019; Alzabeebee, 2019, 2020). In addition, previous studies evaluated the accuracy of Alpha method in predicting the skin friction capacity of bored piles (Cherubini and Vessia, 2007), and Alpha and Beta methods for the case of driven piles (Goh, 1995; Suman et al., 2016). However, Goh (1995) and Suman et al. (2016) did not mention the method used to calculate the α parameter (which is a factor used in the Alpha method to calculate the skin friction capacity of piles embedded in clay) for the case of driven piles, although more than one approach is available in the literature to calculate the α parameter as will be discussed in the next section. In addition, the previous studies did not evaluate the accuracy of the Lambda method, which is also an analytical method to predict the skin friction capacity of piles embedded in clay. Therefore, this study aims to improve the state-of-the-art with respect to the prediction of the skin friction of driven piles by considering two important objectives:

1- The first objective is to use a very powerful and new data driven method to predict the skin friction capacity of driven piles in clay; the method is the multi-objective evolutionary polynomial regression analysis. The strength of this method over the traditional data driven methods is that it has the ability to provide robust and simpler prediction models (Faramarzi, 2011) as the EPR gives the relationship between the parameters in the form of a simple mathematical expression (Ahangar-Asr et al., 2014, 2016, 2018; Alzabeebee et al., 2018, 2019; Nassr et al., 2018a, b). Having an equation as an outcome of the analysis is required to aid future designs and to make it easy to test this equation further when new data becomes available.

2- The second objective is to assess the current analytical methods which have been developed to predict the skin friction capacity of bored piles embedded in

6

172   clay and understand the limitations and the capabilities of these methods, and

173   to compare the prediction capabilities of these methods with the predictions

174   from the multi-objective evolutionary polynomial regression analysis.

175 The methodology of this research is briefly summarized in Figure 1. More details on

176 the methodology will be discussed in Sections 2, 3, 4 and 5.

177 Table 1: Summary of previous studies which have used data driven methods to predict

178 pile settlement and capacity

Reference	Data driven method used	Input parameters	Output of the data driven method	Number of load tests
Shahin (2010)	ANN	D_{eq}, L, D_{stem}, D_{base}, $q_{c_{tip}}$, $q_{c_{shaft}}$ and Fs	Qu	80 load tests for driven piles and 94 load tests for bored piles
Alkroosh and Nikraz (2011a)	GEP	D, L, $q_{c_{tip}}$, $q_{c_{shaft}}$ and Fs	Qu	50 load tests for bored piles and 28 load tests for driven pile
Alkroosh and Nikraz (2011b)	ANN	D, L, $q_{c_{tip}}$, $q_{c_{shaft}}$, $\Delta(\frac{S}{D})$, P_i and P_{i+1}	S/D	50 load tests for bored piles and 30 load tests for driven pile
Ismail and Jeng (2011)	ANN	D, L, P_i, E and k_s	S/D	98
Alkroosh and Nikraz (2012)	GEP	D_{eq}, L, $q_{c_{tip}}$, Fs, $q_{c_{shaft}}$ and E	Qu	25

Alkroosh and Nikraz (2014)	GEP	D, L, N_{shaft}, N_{tip}, St and HE	Qu	25
Momeni et al. (2014)	ANN enhanced with genetic algorithm (GA) optimization technique	L, A, St, W, and H	Qu	50
Shahin (2014a)	RNN	D, L, $q_{c_{tip}}$, Fs, f_{R-tip} and $f_{R-shaft}$	S/D	38
Shahin (2014b)	RNN	D, L, $q_{c_{tip}}$, Fs, f_{R-tip} and $f_{R-shaft}$	S/D	23
Milad et al. (2015)	ANN and GEP	c'_{avg}, $\emptyset'_{avg}$, δ, γ', FPN, L and A	Qu	100
Momeni et al. (2015)	ANN	L, St, A, N_{shaft}, and N_{tip}	fs, Qp and Qu	36
Armaghani et al. (2017)	ANN and hybrid PSO-ANN	Ls/Lr, D, L, UCS and N_{av}	Qu	132
Nejad and Jaksa (2017)	ANN	Type of pile test, type of pile, type of installation, L, A, E, O, $q_{c_{tip}}$, $q_{c_{shaft}}$, Fs and P_i	S/D	56
Harandizadeh et al. (2018a)	ANFIS	L, D, $q_{c_{tip}}$ and Fs	Qu	72

Harandizadeh et al. (2018b)	RBFNN, BR, LM and MT	c'_{avg}, $\emptyset'_{avg}$, δ, γ', FPN, L and A	Qu	100
Moayedi and Hayati (2018a)	FFNNs and FTDNNs	D, L, $q_{c_{tip}}$ and $q_{c_{shaft}}$	S/D	50
Moayedi and Armaghani (2018)	ANN optimised with imperialism competitive algorithm	$\emptyset'_{shaft}$, $\emptyset'_{tip}$, σ'_{tip}, L and A	Qu	59
Shaik et al. (2018)	ANN optimised with imperialism competitive algorithm and neuro-fuzzy inference system	$\emptyset'_{shaft}$, $\emptyset'_{tip}$, σ'_{tip}, L and A	Qu	59
Chen et al. (2019)	neuro-genetic, neuro-imperialism, GEP and ANN	L, A, St, W, and H	Qu	50
Harandizadeh et al. (2019)	ANFIS–GMDH–PSO and FPNN–GMDH	L, D, $q_{c_{tip}}$ and Fs	fs and Qu	72

Note: ANN: artificial neural networks, D_{eq}: driven pile shaft equivalent diameter, L: length of the pile, D_{stem}: bored pile stem diameter, D_{base}: bored pile base diameter, $q_{c_{tip}}$: weighted average cone point resistance over pile tip failure zone, q_{shaft}: weighted average cone point resistance along pile shaft, Fs: weighted average cone sleeve friction resistance, Qu: ultimate pile capacity, GEP: Gene expression programming, D: diameter of the pile, $\Delta(\frac{S}{D})$: normalized settlement increment, P_i:

current load state, P_{i+1}: future load state, S/D: pile settlement to pile diameter, E: modulus of elasticity of the pile, k_s: soil stiffness, , N_{shaft}: average number of blows of the standard penetration test along the pile shaft, N_{tip}: number of blows of the standard penetration test at the pile tip, St: pile set, HE: hammer energy, A: cross-section area of the pile, W: hammer weight, H: hammer drop height, RNN: recurrent neural networks, f_{R-tip}: friction ratio at the pile tip, $f_{R-shaft}$: friction ratio along the pile shaft, c'_{avg}: average effective cohesions of the soil along the pile shaft, $\emptyset'_{avg}$: average angle of shearing resistance along the pile shaft and pile tip, δ: pile-soil friction angle, γ': effective unit weight of the soil, FPN: flap number, fs: skin friction capacity of the pile, Qp: end bearing capacity of the pile, PSO-ANN: artificial numeral network enhanced with particle swarm optimization, Ls/Lr: length of soil layer to socket length, UCS: uniaxial compressive strength, N_{av}: average number of blows based on the standard penetration test the pile shaft and pile tip, O: perimeter of the pile in contact with the soil, ANFIS: neuro-fuzzy inference system, RBFNN: radial basis function neural network, BR: feedforward Bayesian regulation learning algorithm, LM: feedforward Levenberg-Marquardt algorithm, MT: model tree algorithm, FFNNs: feed-forward neural networks, FTDNNs: focused time-delay neural networks, $\emptyset'_{shaft}$: average shearing resistance along the pile shaft, $\emptyset'_{tip}$: average shearing resistance at the pile tip, σ'_{tip}: effective stress at the pile tip, ANFIS–GMDH–PSO: neuro-fuzzy inference system and group method of data handling structure optimized by particle swarm optimization algorithm, FPNN–GMDH: fuzzy polynomial neural network type group method of data handling

213

Start

214

A thorough literature review to identify the gaps in knowledge

215

A thorough literature review on the current analytical methods

216

217

Data collection and processing

218

219

A thorough literature review to develop the evaluation criteria

220

221

Development of a new prediction model using evolutionary polynomial

222

223

Calculation of the performance indices for the developed model

224

225

Calculation of the performance indices for the current analytical methods

226

Conclusions
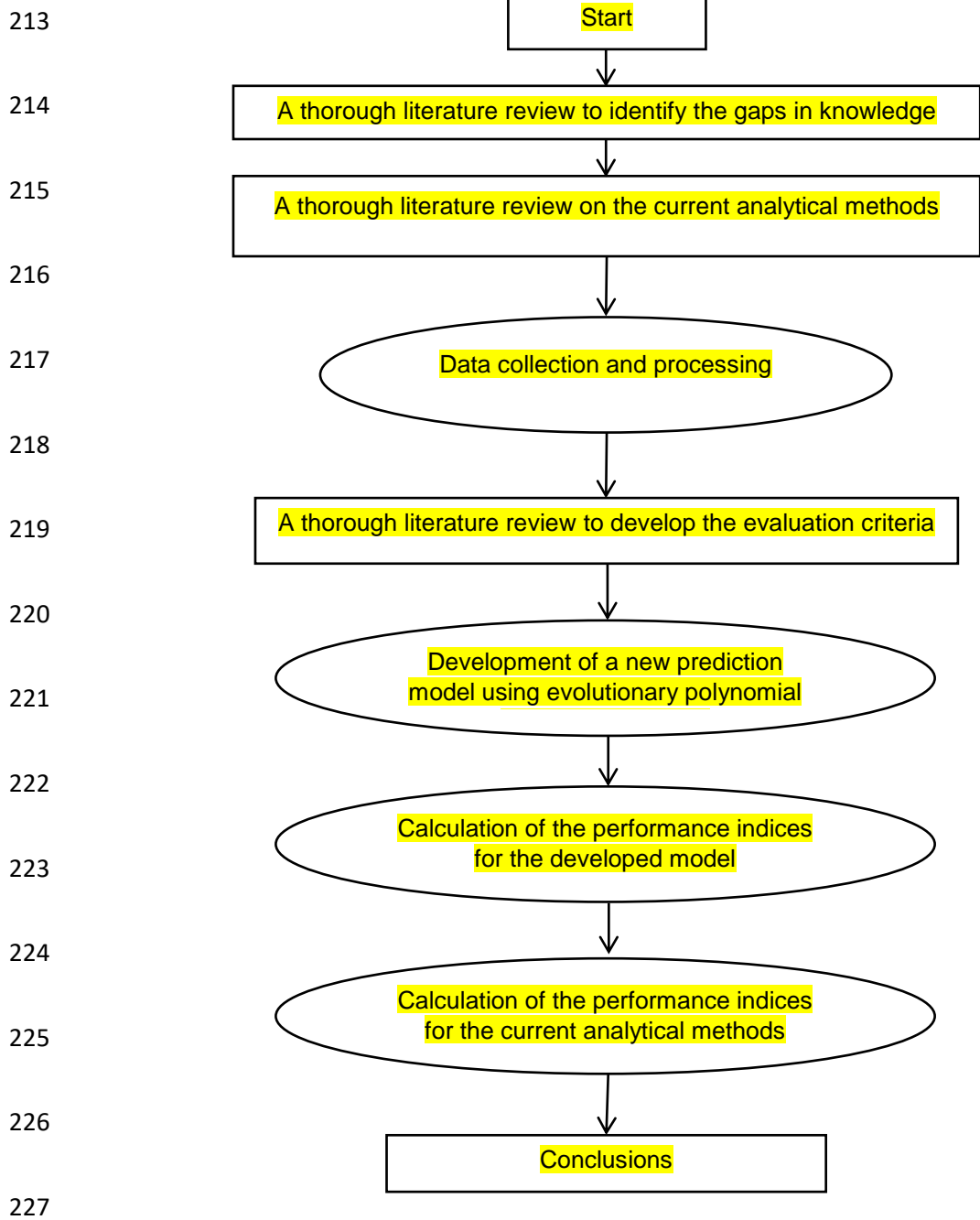
227

228   Figure 1: Flow chart of the methodology of this research

229   **2. Current analytical methods**

230   There are currently three analytical methods available in the literature to estimate the
231   skin friction capacity of driven piles embedded in clay (Das, 2011). These methods
232   are:

233   1- Lambda (λ) method:

234   This method was proposed by Vijayvergiya and Focht (1972) and is based on the idea

235   that the pile driving into the soil induces passive lateral earth pressure (Das, 2011).

236   The method includes the vertical effective stress (σ'_{ave}) and proposes that the skin

237   friction (fs) of the driven pile can be calculated using Equation 1. The λ factor in

238   Equation 1 depends on the embedment depth of the pile (L) as shown in Figure 2.

$$fs = \lambda(\sigma'_{ave} + 2S_u) \tag{1}$$

239   Where, σ'_{ave} is the average vertical effective stress and S_u is the undrained shear

240   strength.
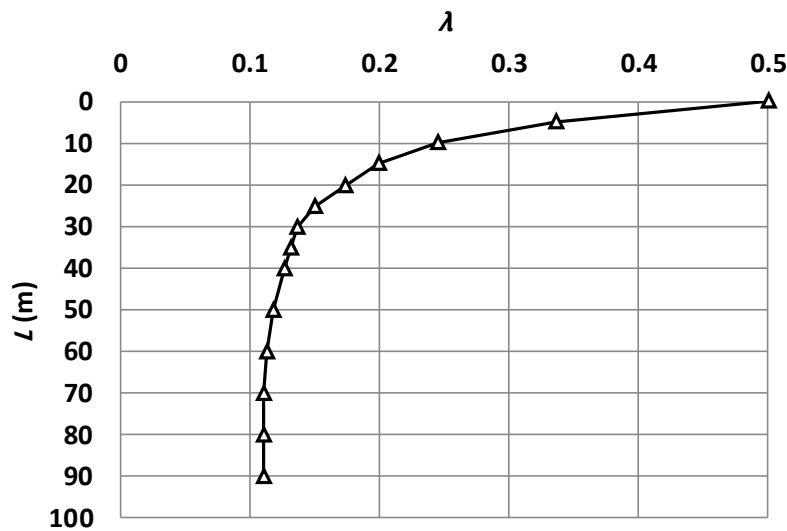
242   Figure 2: Relationship between the λ factor and the embedment depth of the pile (data

243   is from Das (2011))

244   2- Alpha (α) method:

245   This method proposes that the skin friction of a driven pile is a percentage of the

246   undrained shear strength by using an empirical adhesion factor called α as shown in

247   Equation 2. This α empirical factor was originally proposed by Tomlinson in 1957

248   (Terzaghi, 1996). However, there are three methods currently available to estimate

249   the α factor. These methods can be summarized as follows:

250   -   Sladen (1992) method:

251   Sladen (1992) proposed Equation 3 to predict the α coefficient. The C factor in

252   Equation 3 is equal to or greater than 0.5 for driven piles (Das, 2011).

253   -   ISO (2016) method:

254   ISO (2016) suggested two different equations to calculate the α factor

255   depending on the ratio of the undrained shear strength to the average vertical

256   effective stress as shown in Equations 4 and 5.

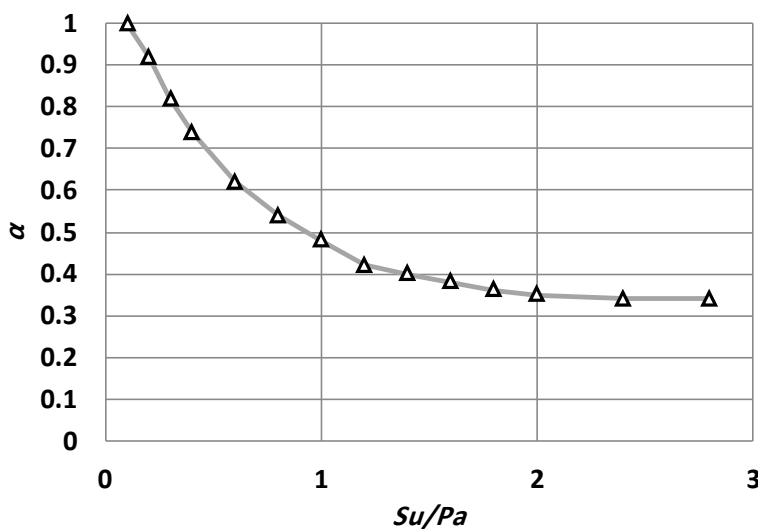257   -   Terzaghi et al. (1996) method:

258   Terzaghi et al. (1996) suggested predicting the α coefficient from Figure 3; Pa

259   in Figure 3 is the atmospheric pressure (100 kPa). This Figure has been

260   developed based on data collected from Dennis and Olson (1983) and Stas

261   and Kulhawy (1984). However, Terzaghi et al. (1996) also recommended

262   multiplying the α coefficient obtained from Figure 3 by 0.54 (i.e. a reduction

263   factor) for piles with a length equal to or greater than 50 m. Also, for pile lengths

264   from 30 m to 50 m, the reduction factor varies linearly between 1.00 and 0.56.

$$fs = \alpha S_u \tag{2}$$

$$\alpha = C\left(\frac{\sigma'_{ave}}{S_u}\right)^{0.45} \tag{3}$$

$$\alpha = 0.5\left(\frac{S_u}{\sigma'_{ave}}\right)^{-0.5} \quad \text{for } \frac{S_u}{\sigma'_{ave}} \leq 1 \tag{4}$$

$$\alpha = 0.5\left(\frac{S_u}{\sigma'_{ave}}\right)^{-0.25} \quad \text{for } \frac{S_u}{\sigma'_{ave}} > 1 \tag{5}$$

265

266   Figure 3: The α factor based on Terzaghi et al. (1996)

267   3- Beta (β) method

268 This method considers a different approach compared to the other two methods. In
269 this method, the skin friction is determined using the drained angle of internal friction
270 of the remolded clay (ϕ') as shown in Equations 6 to 9 (Das, 2011). The beta factor
271 ranges between 0.25 to 0.4 (Goh, 1995).

$$fs = \beta \sigma'_{ave} \tag{6}$$
$$\beta = K \tan \phi' \tag{7}$$
$$K = 1 - \sin \phi' \quad \text{for normally consolidated clay} \tag{8}$$
$$K = (1 - \sin \phi')\sqrt{OCR} \quad \text{for over consolidated clay} \tag{9}$$

272 Where, OCR is the over-consolidation ratio.

3. Data used in the analyses

273

274 The data used in the current study have been adapted from a database of skin friction
275 capacities of driven piles presented by Goh (1995). The database comprises 65 points
276 of data on the skin friction capacity of driven piles (fs). In addition, the data contains
277 the length of the pile (L), the diameter of the pile (D), the average vertical effective
278 stress (σ'_{ave}) and the average undrained shear strength (S_u). Goh (1995) developed
279 this database by collecting results from the literature; these results were for pile load
280 tests conducted on timber and steel pipe piles. It is worth mentioning that these
281 parameters have been selected as they are the most influential parameters with
282 respect to the skin friction capacity of the pile. These parameters have also been used
283 in previous studies for the prediction of the skin friction capacity of piles (Goh, 1995,
284 Samui, 2008, 2011, 2019, Suman et al., 2016, Prayogo, 2018, Moayedi and Hayati,
285 2018b).

286 Table 2 shows the mean, standard deviation, maximum value (Max.), minimum value
287 (Min.) and range of the collected data.

288

289

290   Table 2: Statistics of the data used in this study

Statistic indicator	Parameter				
	L (m)	D (cm)	σ'_{ave} (kPa)	S_u (kPa)	fs (kPa)
Mean	21.55	31.45	124.58	62.16	40.85
Standard deviation	16.37	16.61	127.71	60.03	36.52
Max.	96.00	76.70	718.00	335.00	192.10
Min.	4.60	11.40	19.00	9.00	8.00
Range	91.40	65.30	699.00	326.00	184.10

291   **4. Multi-objective evolutionary polynomial regressions analysis (EPR)**

292   Multi-Objective Evolutionary Polynomial Regression (MOGA-EPR) is a genetic
293   algorithm-based regression analysis developed by Giustolisi and Savic (2009) based
294   on the original evolutionary polynomial regression analysis developed by Giustolisi
295   and Savic (2006). The methodology of MOGA-EPR is based on using a genetic
296   algorithm in combination with a regression analysis (Alzabeebee et al., 2018, 2019;
297   Alzabeebee, 2019, 2020). In this method, the 'fitting' is conducted utilizing the least
298   square method and the selection of the best fitting model is done using the genetic
299   algorithm. The MOGA-EPR controls the model fitness and model complexity using
300   spread functions to enable more robust analyses (Giustolisi and Savic, 2009). This
301   method also controls overfitting issues by using penalization procedures.

302   Equation 10 presents the starting point of the MOGA-EPR (Giustolisi and Savic, 2006).
303   This equation produces an over-determined system, which is solved based on the
304   least square methodology (Giustolisi and Savic, 2006).

$$y = \sum_{j=1}^{m} F\big(X, f(X), a_j\big) + a_0 \tag{10}$$

305   Where y is the estimated output skin friction, a_j is a constant value, F is an assumed
306   governing function between the input and the output variables; this function develops
307   as the analysis time increases and based on artificial intelligence. X represents the
308   independent variables matrix, f is the general form of the output function and m is the

15

309 maximum number of terms in the produced equation and it is set by the user, and a_0

310 is the bias.

311 After solving Equation 10, the MOGA-EPR is formulated to find the model, which

312 provides the best fit to the data by using different combinations of the exponents with

313 the aid of artificial intelligence. Finally, the performance of the developed model is

314 judged by determining a coefficient called the coefficient of determination (CD) and the

315 model which scores the highest CD is selected; the CD is determined using Equation

316 11 (Alani et al., 2014a, b; Faramarzi et al., 2014). It is worth noting that the exponents

317 considered in the EPR analysis are also controlled by the user. More information on

318 the MOGA-EPR can be found in Alani et al. (2014); Faramarzi et al. (2014); Ahangar-

319 Asr et al. (2014) and Alzabeebee (2017).

$$CD = 1 - \frac{\sum_N \left(fs_{(m)} - fs_{(p)}\right)^2}{\sum_N (fs_{(m)} - \frac{1}{N}\sum_N fs_{(p)})^2} \tag{11}$$

320 Where, $fs_{(m)}$ is the measured skin friction, $fs_{(p)}$ is the predicted skin friction, and N is

321 the number of the input data used in the development of the model.

5. Criteria considered to evaluate the accuracy of the MOGA-EPR model and the analytical methods

324 The quality of the prediction of the MOGA-EPR model and the available analytical

325 methods have been assessed following a statistical based methodology similar to

326 previous studies (Ozer et al., 2008; Alkroosh et al., 2014, 2015; Onyejekwe et al.,

327 2015; Huang et al., 2019). The following points summarize the statistical measures

328 used in the evaluation methodology:

329 1- The first statistical measure was based on finding the error in the prediction by

330 calculating the mean absolute error (MAE) and the root mean square error

331 (RMSE). Equations 12 and 13 show the mathematical formulation of the MAE

332 and the RMSE (Ozer et al., 2008; Onyejekwe et al., 2015; Huang et al., 2019).

333 The lower the MAE and the RMSE, the better the prediction. It is worth

334 mentioning that the MAE has been considered because it provides insight into

335 the average error of the prediction. In addition, the RMSE has been considered

16

336   because it provides useful insight into the large error of the prediction, as the
337   errors are squared before they are averaged as can be clearly noted in
338   Equation 13 (Ashtiani et al., 2018).

$$MAE = \frac{1}{n}\sum_{1}^{n}\left|fs_{(p)} - fs_{(m)}\right| \tag{12}$$

$$RMSE = \sqrt{\frac{1}{n}\Sigma_{1}^{n}\left(fs_{(p)} - fs_{(m)}\right)^{2}} \tag{13}$$

339 Where, n is the number of data points used in the evaluation; $fs_{(p)}$ is the predicted
340 skin friction of the pile; and $fs_{(m)}$: is the skin friction measured in the field.

341   2- The second statistical measure was based on calculating the mean (μ) of the
342   ratio of the predicted skin friction to the measured skin friction as shown in
343   Equation 14 (Onyejekwe et al., 2015). The expected range of the mean is zero
344   to infinity. However, the optimum prediction should score a mean equal to 1
345   (Onyejekwe et al., 2015). The predictive model underestimates the skin friction
346   if the mean is less than one and overestimates the skin friction if the mean is
347   higher than one.

$$\mu = \frac{1}{n}\sum_{1}^{n}\left(\frac{fs_{(p)}}{fs_{(m)}}\right) \tag{14}$$

348   3- The third statistical measure was the standard deviation (σ) of the predicted
349   skin friction to the measured skin friction. The standard deviation is calculated
350   using Equation 15. The standard deviation provides a good indication to the
351   distribution of the predicted values around the mean. The range of the standard
352   deviation is between zero and one. A zero value provides the optimum
353   prediction in which the scatter of the prediction around the mean a minimum.
354   However, a value of one means a maximum scatter around the mean. Hence,
355   the closer the standard deviation is to zero, the better the prediction (Alkroosh
356   and Nikraz, 2014).

$$\sigma = \sqrt{\frac{\sum_1^n \left(\frac{fs_{(p)}}{fs_{(m)}} - \mu\right)^2}{n-1}} \tag{15}$$

357   4- The fourth statistical measure was the coefficient of determination (R^2). The R^2

358   measures the average error of the prediction. The R^2 ranges between zero and

359   one, with an optimum value of one. Hence, the closer R^2 is to one, the better

360   the prediction accuracy (Alzabeebee et al. 2017; Tinoco et al. 2019). R^2 is

361   calculated using Equation 16 (Mohammadzadeh et al., 2019).

$$R^2 = \frac{\sum_{i=1}^n (fs_{(p)_i} - fs_{(p)\,average})(fs_{(m)_i} - fs_{(m)\,average})}{\sqrt{\sum_{i=1}^n (fs_{(p)_i} - fs_{(p)\,average})^2 \sum_{i=1}^n (fs_{(m)_i} - fs_{(m)\,average})^2}} \tag{16}$$

362 Where, $fs_{(p)\,average}$ is the average of the predicted skin friction values and $fs_{(m)\,average}$

363 is the average of the measured skin friction values.

364   5- The fifth statistical measure was the variance account for (VAF). The VAF is

365   usually employed to check the correctness of the predictive model. This is done

366   by comparing the measured and the predicted output using Equation 17

367   (Armaghani et al., 2017). A VAF value of 100 means that the predictive model

368   provides a perfect estimation of the output. Therefore, the closer the VAF of the

369   predictive model to 100, the better the prediction (i.e. lower variance).

$$VAF = \left[1 - \frac{var(fs_{(m)} - fs_{(p)})}{var(fs_{(m)})}\right] \times 100 \tag{17}$$

370   6- The final statistical measure was the $a20-index$. This statistical measure

371   evaluates the percentage of the predictive outputs that falls within the range of

372   80% to 120% of the measured output. A value of the $a20-index$ of 1.0 means

373   that the predictions of the models are equal to, or below, a 20% error. In

374   addition, the closer the $a20-index$ is to 1 the better, as it means that there are

375   many predictions that are equal to, or below, a 20% error. The $a20-index$ is

376   calculated using Equation 18 (Armaghani, 2020).

$$a20 - index = \frac{m20}{n} \tag{18}$$

377 Where, $m20$ is the number of results where the predicted to the measured skin friction
378 is between 0.8 to 1.2.

6. Development of the MOGA-EPR model

380 The data, with statistics shown in Table 2, has been used to develop the MOGA-EPR
381 model. This data has been divided into two groups: training data and testing data. 80%
382 of the data has been used in the model development (training stage) and 20% of the
383 data has been used in the model testing and validation (testing stage). It should be
384 noted that dividing the data into training and test data is common in the development
385 of data driven models, i.e. the training data is used in the training and the development
386 of the MOGA-EPR model, and the performance of the developed model has been
387 checked using independent data that has not been used in the training stage. Hence,
388 the use of testing data ensures the robustness and accuracy of the developed model
389 (Alani et al., 2014a, b; Faramarzi et al., 2014; Ahangar-Asr et al., 2014; Alzabeebee,
390 2017, 2019, 2020; Alzabeebee et al., 2018, 2019). However, to avoid model
391 extrapolation the variables of the testing data should be in the range of the data used
392 in the model training (i.e. model development) (Alzabeebee, 2017, 2019, 2020;
393 Alzabeebee et al., 2018, 2019). Hence, the data have been randomly shuffled and
394 divided into two group, then statistical analyses have been conducted to ensure that
395 the training and testing data are consistent. Tables 3 and 4 show the mean, standard
396 deviation, maximum value (Max.), minimum value (Min.) and the range of both the
397 training and testing data, respectively. The tables demonstrate the consistency of the
398 training and the validation data.

399 The MOGA-EPR analysis was conducted after ensuring that the data are consistent.
400 Several structures and exponents of the mathematical model are now examined, and
401 the performance of the obtained model is also studied using the criteria discussed
402 previously in this paper. Equation 18 shows the best mathematical model obtained
403 from the MOGA-EPR analysis. Figures 4a, b, c, d, e, f and g show the obtained MAE,
404 $RMSE$, μ, σ, R^2, VAF and $a20 - index$ values for the training and testing data,
405 respectively. Figure 4a clearly shows that the developed MOGA-EPR model gives a

very good accuracy with a MAE of 3.4 and 4.2 for the training and testing data, respectively. The obtained $RMSE$ results presented in Figure 4b also show that the model offers a very good prediction, where the $RMSE$ is equal to 4.6 and 5.3 for the training and testing data, respectively. The μ values shown in Figure 4c give additional proof of the accuracy, where the developed model slightly overestimates the skin friction as the obtained μ values are 1.03 and 1.12 for the training and testing data, respectively. Furthermore, the obtained values of the σ (Figure 4d) and R^2 (Figure 4e) also show the strength of the model, where σ is equal to 0.24 for the training and 0.15 for the testing data and R^2 is very close to one being equal to 0.98 and 0.91 for the training and the testing data, respectively. The results of the VAF (Figure 4f) provides additional trust in the robustness of the model as the obtained VAF is very close to 100 for training and testing data (99 for training data and 97 for testing data). The $a20 - index$ analyses (Figure 4g) also demonstrate the prediction capabilities of the models as the percentage of the obtained predictions with error less than or equal to 20% is 75% and 77% for training and testing data, respectively.

$$fs = 28.44\frac{D.\sqrt{S_u}}{L^3} - 3\times10^{-7}\frac{\sqrt{D}.\sqrt{\sigma'_{ave}}.{S_u}^3}{L^2} - 83.81\frac{\sqrt{D}}{\sqrt{L}.\sqrt{\sigma'_{ave}}}$$
$$+ 0.023\frac{\sqrt{D}.\sqrt{\sigma'_{ave}}.S_u}{\sqrt{L}} + 27.17 \tag{18}$$

Figures 5a and b show the relationship between the predicted and measured skin friction values. It is clear from the figures that most of the points are on or very close to the no-error line, which means that the developed model provides very good prediction and providing further confidence in the developed MOGA-EPR model.

430   Table 3: Statistics of the training data used in the MOGA-EPR analysis

| Statistical indicator	Parameter				
	L (m)	D (cm)	σ'_{ave} (kPa)	S_u (kPa)	fs (kPa)
Mean	20.56	30.80	119.57	63.13	41.80
Standard deviation	16.44	17.12	132.08	63.65	38.38
Max.	96.00	76.70	718.00	335.00	192.10
Min.	4.60	11.40	19.00	9.00	8.00
Range	91.40	65.30	699.00	326.00	184.10

431

432

433   Table 4: Statistics of the testing data used in the MOGA-EPR analysis

| Statistical indicator	Parameter				
	L (m)	D (cm)	σ'_{ave} (kPa)	S_u (kPa)	fs (kPa)
Mean	25.52	34.05	144.62	58.31	37.03
Standard deviation	16.08	14.69	110.94	44.50	28.83
Max.	66.40	61.00	448.00	185.00	109.20
Min.	9.40	15.00	49.00	17.00	12.00
Range	57.00	46.00	399.00	168.00	97.20

434

(a)

(b)

(c)

(d)

(e)

(f)

(g)
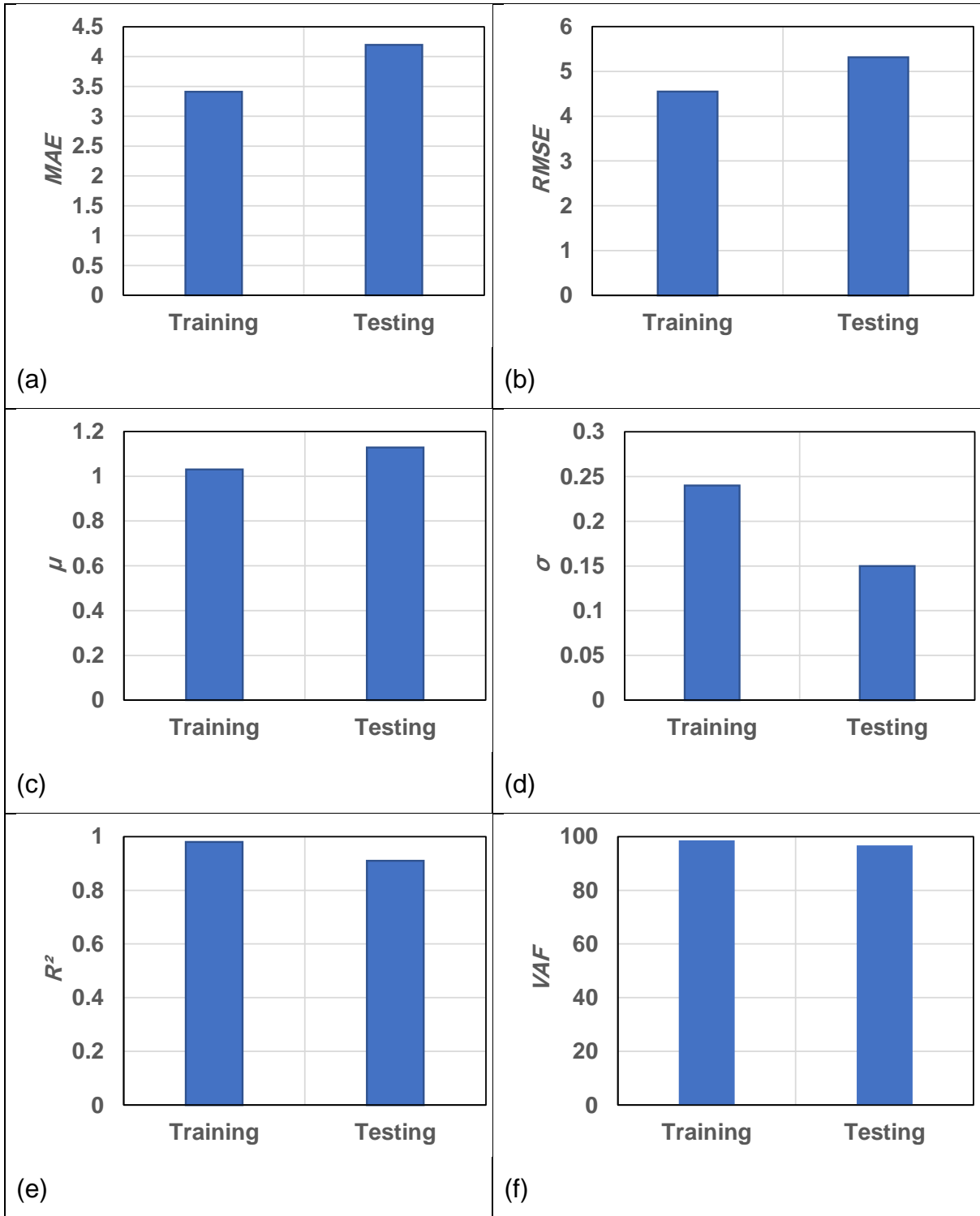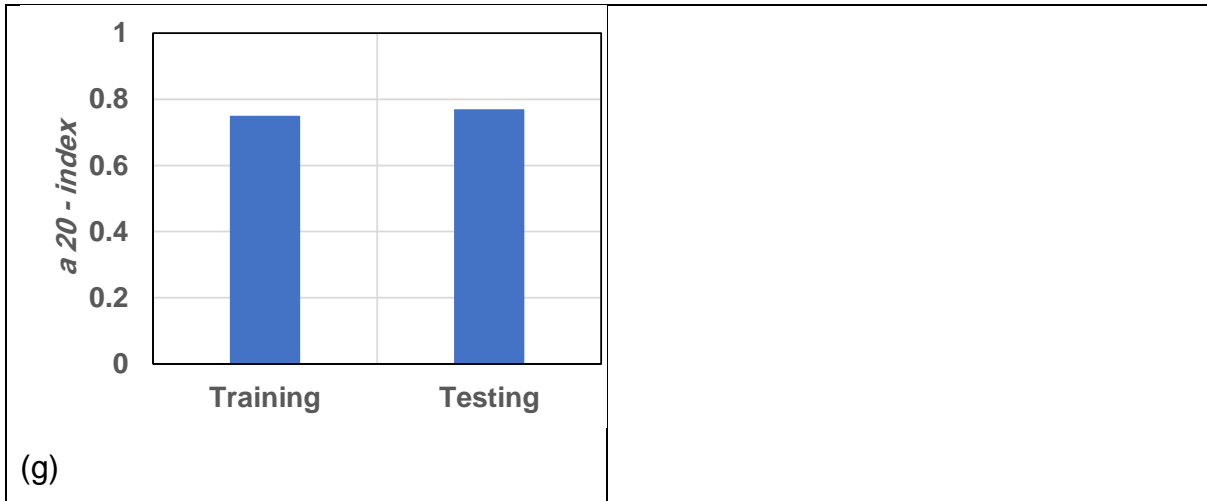
Figure 4: Results of the statistical analyses of the MOGA-EPR model: (a) Mean absolute error (MAE); (b) root mean square error ($RMSE$); (c) Mean (μ); (d) standard deviation (σ); (e) coefficient of determination (R^2); (f) variance account for (VAF); and (g) $a20 - index$

(a)

(b)
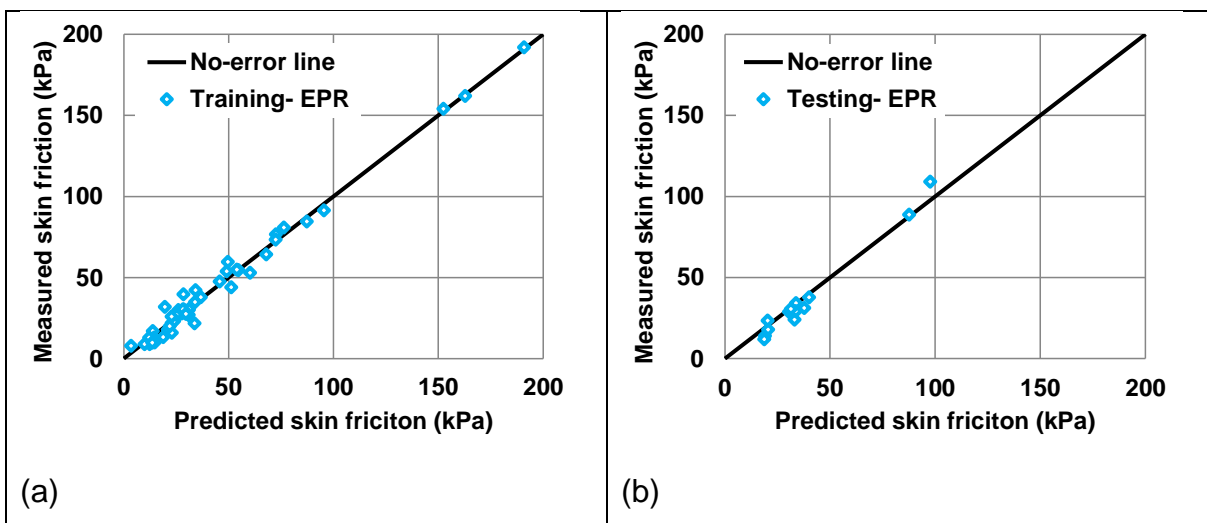
Figure 5: Relationship between the MOGA-EPR predicted skin friction and measured skin friction for: (a) training data; and (b) testing data

7. Evaluation of the accuracy of the analytical methods

It is very important to understand the limitations and the accuracy of the current analytical methods. Thus, the accuracy of the previously discussed analytical methods has been assessed in this section using the assessment methodology discussed

earlier in this paper. The results of the assessment have also been compared with the MOGA-EPR model. The β factor has been considered equal to 0.33 in the calculation of the skin friction capacity using the Beta method; this value is the average of the expected range for the β factor (Goh, 1995). Furthermore, the three methods mentioned previously to calculate the α factor have been considered in this assessment; the Sladen (1992) method has been named Alpha 1, the ISO method has been named Alpha 2, and the Terzaghi et al. method has been named Alpha 3.

Figures 6a, b, c, d, e, f and g show the obtained MAE, $RMSE$, μ, σ, R^2, VAF and $a20 - index$ for all of the analytical methods, respectively. In addition, Figures 7a, b, c, d and e show the relationship of the predicted and measured skin friction for all of the analytical methods. Comparing Figures 6 and 7 with Figures 4 and 5 clearly shows the MOGA-EPR model predicts the skin friction capacity better than all of the other analytical methods. Furthermore, Figure 6 shows that the Lambda method predicted the skin friction with lowest error (Figures 6a and b), lowest standard deviation (Figure 6d), highest coefficient of determination (Figure 6e), highest value for the variance account for (Figure 6f) compared with the Alpha and Beta methods. However, the mean (μ) of the Lambda method was relatively higher than the other methods (Figure 6c). Furthermore, the results of the mean (μ) show that, on average, all the analytical methods tend to overestimate the skin friction of the pile except for the Alpha 3 method which, on average, slightly underestimates the skin friction capacity. In addition, Figure 6g reveals that on average the Lambda, Alpha 1 and Alpha 2 methods produces similar accuracy in terms of the percentage of the predictions with error equal to or lower than 20%, where the scored $a20 - index$ value is equal to 0.60, 0.62 and 0.63 for Lambda, Alpha 1 and Alpha 2 methods, respectively. Figures 7a, b, c, d and e show that Lambda method provides less scatter around the mean compared with the Alpha and Beta methods and this is confirmed by the obtained coefficient of determination and VAF, which is higher for the Lambda method as shown in Figures 6e and f.

It is also obvious from Figure 6 that the Alpha 1 and Alpha 2 methods predict the skin friction capacity with slightly higher MAE (8.9 for Alpha 1 and 8.1 for Alpha 2), $RMSE$ (14.4 for Alpha 1 and 13.0 for Alpha 2) and σ (0.32 for Alpha 1 and 0.27 for Alpha 2) compared than the Lambda method. In addition, the Alpha 1 and Alpha 2 methods predict the skin friction capacity with slightly lower R^2 (0.85 for Alpha 1 and 0.88 for

479 Alpha 2) and VAF (85 for Alpha 1 and 88 for Alpha 2) than the Lambda method. The
480 Alpha 1 and Alpha 2 methods also achieved a μ value closer to 1 ($\mu = 1.02$ for the
481 Alpha 1 method and $\mu = 1.07$ for the Alpha 2 method) compared with the Lambda
482 method ($\mu = 1.16$). Thus, the Alpha 1 and Alpha 2 methods can be both ranked second
483 compared with other analytical methods.

484 Finally, Figures 6 and 7 also show that the Beta method is the worst performing
485 method and the error produced using this method is very high ($MAE = 17.2$ and
486 $RMSE = 28.0$) compared with other methods. Also, the σ value obtained using the Beta
487 method is 1.00; this means a maximum scatter around the mean and can also be
488 confirmed by the very low coefficient of determination calculated using this method,
489 which is equal to 0.55 (Figure 6e) and the very low VAF, which is equal to 40 (Figure
490 6f). The very low coefficient of determination of the Beta method can also be evidenced
491 by Figure 7e, which shows a large scatter of the predicted-measured relationship
492 compared with the no-error line. Also, the $a20 - index$ for the Beta method is very low
493 and is equal to 0.37; this means only 37% of the predictions are with error equal to or
494 less than 20%. Hence, the Beta method ranked last based on this assessment.

(a) (b)
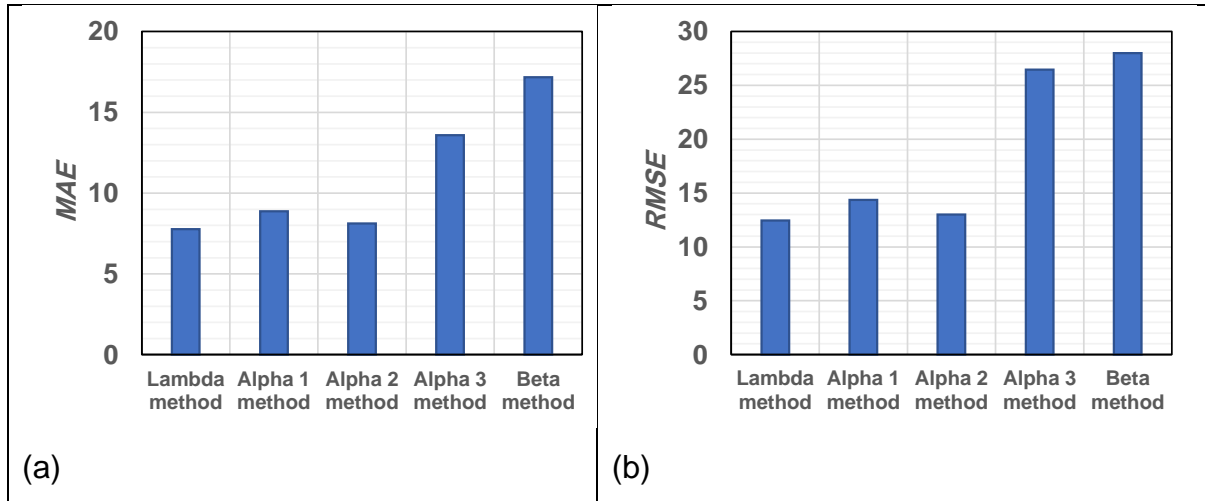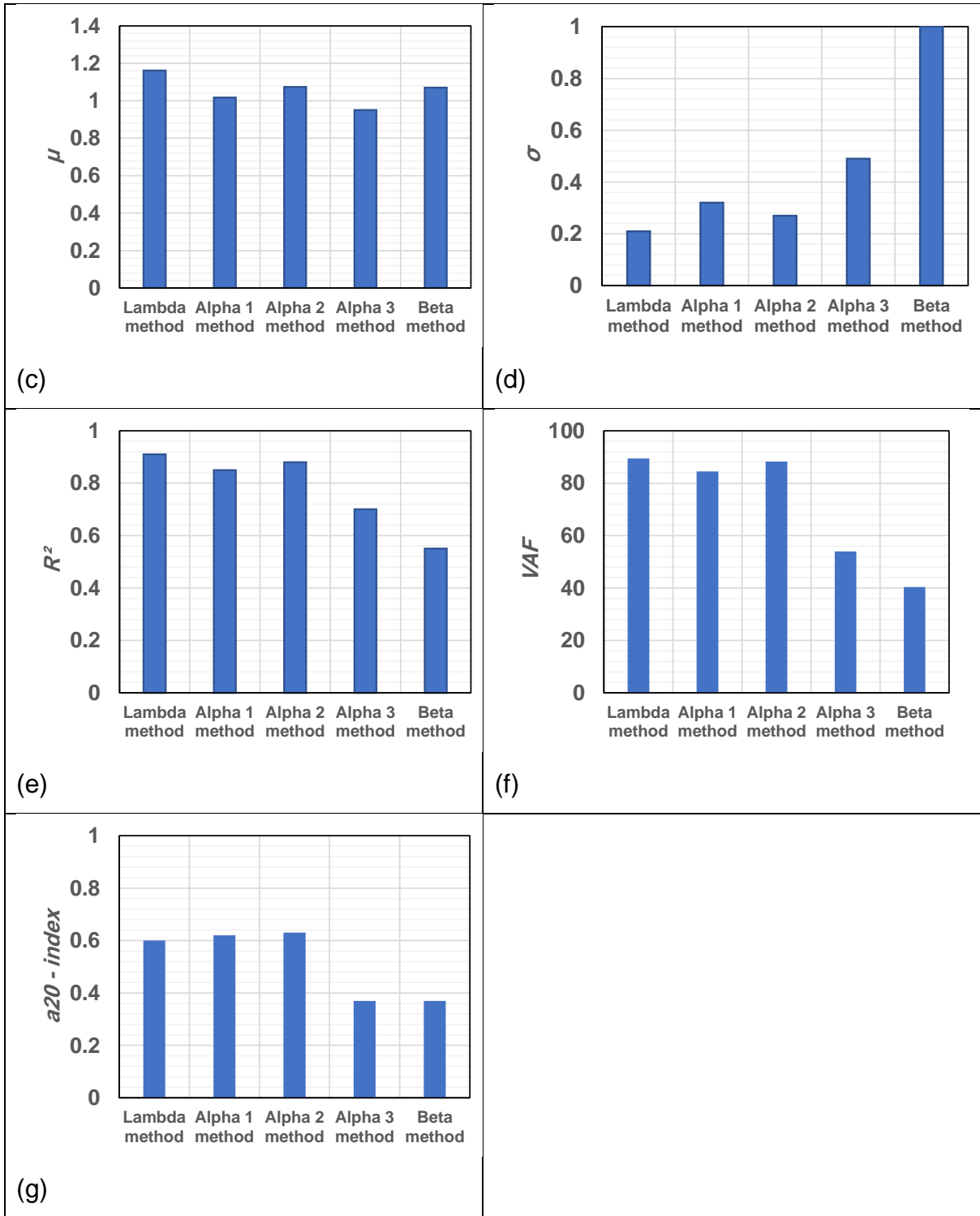
Figure 6: Results of the statistical analysis: (a) Mean absolute error (MAE); (b) root mean square error ($RMSE$); (c) Mean (μ); (d) standard deviation (σ); and (e) coefficient of determination (R^2); (f) Variance account for (VAF); and (g) $a20 - index$

(a)

(b)

(c)

(d)

(e)
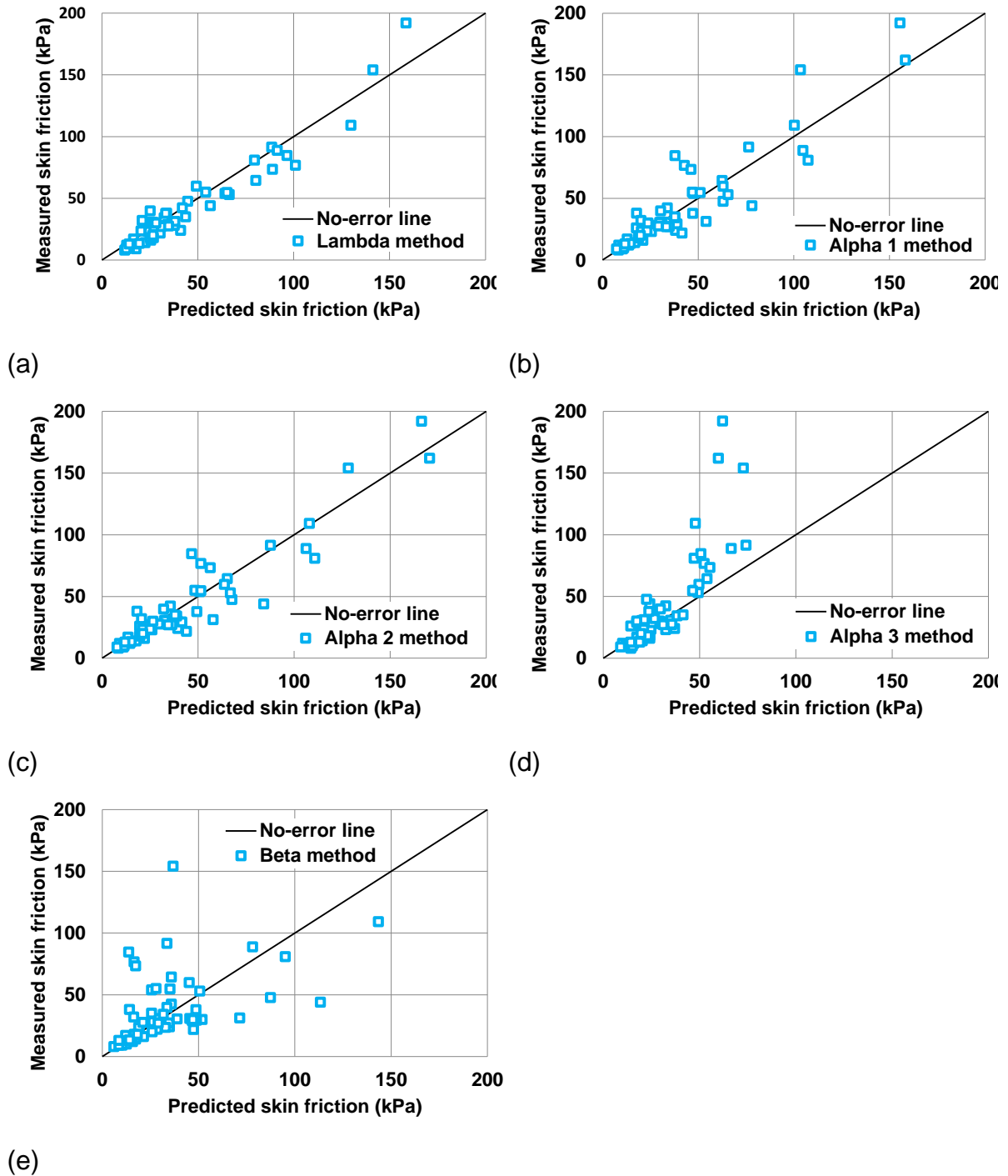
498   Figure 7: Predicted versus measured skin friction using: (a) Lambda method; (b) Alpha

499   1 method; (c) Alpha 2 method; (d) Alpha 3 method; and (e) Beta method

500   **8. Conclusions**

501   The results of this study have demonstrated the abilities of the multi-objective

502   evolutionary (MOGA-EPR) polynomial regression analysis in predicting the skin

503   friction capacity of driven piles embedded in clay. The MOGA-EPR model achieved a

very low error, a mean value close to 1, low standard deviation, very high coefficient of determination, very high value for the variance account for and high value for the $a20 - index$ for both training and testing data. Furthermore, the accuracy of the MOGA-EPR model has been confirmed by presenting the relationship between the predicted and measured skin friction values for both the training and testing data and the presented relationships demonstrated the accuracy of the MOGA-EPR model as most of the points were on or very close to the no-error line for both the testing and training data. In addition, the MOGA-EPR model has been compared with the available analytical methods in the literature and the results have demonstrated that the developed model is better than the available analytical methods as the MOGA-EPR model performed better based on the statistical measures. Thus, the developed model can be used with confidence in future designs. However, it is worth stating that the developed model has been trained and tested based on lengths of pile ranging from 4.60 m to 96.00 m, diameters of piles ranging from 11.40 cm to 76.70 cm and undrained cohesion ranging from 9.00 kPa to 355 kPa. Hence, the model should be used for designs within these ranges. Nonetheless, the developed model can also be tested further in the future when new data becomes available.

In addition, assessing the available analytical methods showed that the Lambda method is the most accurate method compared with Alpha and Beta methods. This method scored an mean absolute error (MAE) of 7.8, a root mean square error ($RMSE$) of 12.5, a mean (μ) of 1.16, a standard deviation (σ) of 0.21, a coefficient of determination (R^2) of 0.91, a value for the variance account for (VAF) of 89 and $a20 - index$ of 0.6. Hence, this method can also be used as an alternative to the MOGA-EPR model developed in this study. Furthermore, the Alpha 1 method (Sladen, 1992) and Alpha 2 method (ISO, 2016) also scored low errors and high coefficient of determination; the errors of both methods are slightly higher than the Lambda method. The Alpha 1 and Alpha 2 methods also scored a μ closer to 1 than the Lambda method; therefore, both methods can be ranked second. The Beta method scored lowest compared with the other analytical methods with a MAE of 17.2, a $RMSE$ of 28.0, a μ of 1.07, a σ of 1.00, a R^2 of 0.55, a VAF of 40 and $a20 - index$ of 0.37. The developed mathematical model in this paper and the results of the assessment of the analytical methods are very useful to geotechnical engineers and will help to achieve better pile designs in the future.

537   **References**

538   Ahangar-Asr, A. and Javadi, A.A., 2016. Air losses in compressed air tunneling: a
539   prediction model. Proceedings of the ICE-Engineering and Computational Mechanics,
540   169(3), pp.140-147.

541   Ahangar-Asr, A., Faramarzi, A. and Javadi, A.A., 2018. An evolutionary modelling
542   approach to predicting stress-strain behaviour of saturated granular soils. Engineering
543   Computations, 35(8), pp.2931-2952.

544   Ahangar-Asr, A., Javadi, A.A., Johari, A. and Chen, Y., 2014. Lateral load bearing
545   capacity modelling of piles in cohesive soils in undrained conditions: an intelligent
546   evolutionary approach. Applied Soft Computing, 24, pp.822-828.

547   Alani, A.M. and Faramarzi, A., 2014b. An evolutionary approach to modelling
548   concrete degradation due to sulphuric acid attack. Applied Soft Computing, 24,
549   pp.985-993.

550   Alani, A.M., Faramarzi, A., Mahmoodian, M. and Tee, K.F., 2014a. Prediction of
551   sulphide build-up in filled sewer pipes. Environmental technology, 35(14), pp.1721-
552   1728.

553   Alavi, A.H. and Sadrossadat, E., 2016. New design equations for estimation of ultimate
554   bearing capacity of shallow foundations resting on rock masses. Geoscience
555   Frontiers, 7(1), pp.91-99.

556   Alkroosh, I. and Nikraz, H., 2011a. Correlation of pile axial capacity and CPT data
557   using gene expression programming. Geotechnical and Geological Engineering,
558   29(5), pp.725-748.

559   Alkroosh, I. and Nikraz, H., 2011b. Simulating pile load-settlement behavior from
560   CPT data using intelligent computing. Central European Journal of Engineering, 1(3),
561   pp.295-305.

562   Alkroosh, I. and Nikraz, H., 2012. Predicting axial capacity of driven piles in cohesive

563   soils using intelligent computing. Engineering Applications of Artificial Intelligence,

564   25(3), pp.618-627.

565   Alkroosh, I. and Nikraz, H., 2014. Predicting pile dynamic capacity via application of

566   an evolutionary algorithm. Soils and Foundations, 54(2), pp.233-242.

567   Alkroosh, I.S., Bahadori, M., Nikraz, H. and Bahadori, A., 2015. Regressive approach

568   for predicting bearing capacity of bored piles from cone penetration test data. Journal

569   of Rock Mechanics and Geotechnical Engineering, 7(5), pp.584-592.

570   Alzabeebee, S., 2017. Enhanced design approaches for rigid and flexible buried pipes

571   using advanced numerical modelling. PhD Thesis, University of Birmingham, United

572   Kingdom.

573   Alzabeebee, S., 2019. Seismic response and design of buried concrete pipes

574   subjected to soil loads. Tunnelling and Underground Space Technology, 93,

575   p.103084.

576   Alzabeebee, S., 2020. Dynamic response and design of a skirted foundation

577   subjected to vertical vibration. Geomechanics and Engineering, 20(4), pp. 345-358.

578   Alzabeebee, S., Chapman, D., Jefferson, I. and Faramarzi, A., 2017. The response

579   of buried pipes to UK standard traffic loading. Proceedings of the Institution of Civil

580   Engineers-Geotechnical Engineering, 170(1), pp.38-50.

581   Alzabeebee, S., Chapman, D.N. and Faramarzi, A., 2018. Development of a novel

582   model to estimate bedding factors to ensure the economic and robust design of rigid

583   pipes under soil loads. Tunnelling and Underground Space Technology, 71, pp.567-

584   578.

585   Alzabeebee, S., Chapman, D.N. and Faramarzi, A., 2019. Economical design of buried

586   concrete pipes subjected to UK standard traffic loading. Proceedings of the Institution

587   of Civil Engineers-Structures and Buildings, 172(2), pp.141-156.

588 Armaghani, D.J., Asteris, P.G., Askarian, B., Hasanipanah, M., Tarinejad, R. and
589 Huynh, V.V., 2020. Examining Hybrid and Single SVM Models with Different Kernels
590 to Predict Rock Brittleness. Sustainability, 12(6), p.2229.

591 Armaghani, D.J., Mohamad, E.T., Narayanasamy, M.S., Narita, N. and Yagiz, S.,
592 2017. Development of hybrid intelligent models for predicting TBM penetration rate in
593 hard rock condition. Tunnelling and Underground Space Technology, 63, pp.29-43.

594 Armaghani, D.J., Raja, R.S.N.S.B., Faizi, K. and Rashid, A.S.A., 2017. Developing a
595 hybrid PSO–ANN model for estimating the ultimate bearing capacity of rock-socketed
596 piles. Neural Computing and Applications, 28(2), pp.391-405.

597 Ashtiani, R.S., Little, D.N. and Rashidi, M., 2018. Neural network based model for
598 estimation of the level of anisotropy of unbound aggregate systems. Transportation
599 Geotechnics, 15, pp.4-12.

600 Chen, W., Sarir, P., Bui, X.N., Nguyen, H., Tahir, M.M. and Armaghani, D.J., 2019.
601 Neuro-genetic, neuro-imperialism and genetic programing models in predicting
602 ultimate bearing capacity of pile. Engineering with Computers, DOI:
603 https://doi.org/10.1007/s00366-019-00752-x.

604 Cherubini, C. and Vessia, G., 2007. Reliability approach for the side resistance of
605 piles by means of the total stress analysis (α Method). Canadian Geotechnical
606 Journal, 44(11), pp.1378-1390.

607 Das, B., 2011. Principles of Foundations Engineering, Seventh edition, Cengage
608 Learning.

609 Dennis, N.D. and Olson, R.E., 1983. Axial capacity of steel pipe piles in clay. In From
610 Soil Behavior Fundamentals to Innovations in Geotechnical Engineering: Honoring
611 Roy E. Olson (pp. 176-194). ASCE.

612 Doherty, P. and Gavin, K., 2011. The shaft capacity of displacement piles in clay: a
613 state of the art review. Geotechnical and Geological Engineering, 29(4), pp.389-410.

614   Faramarzi, A., 2011. Intelligent computational solutions for constitutive modelling of
615   materials in finite element analysis. PhD. Thesis, University of Exeter, United
616   Kingdom.

617   Faramarzi, A., Alani, A.M. and Javadi, A.A., 2014. An EPR-based self-learning
618   approach to material modelling. Computers & Structures, 137, pp.63-71.

619   Fiore, A., Quaranta, G., Marano, G.C. and Monti, G., 2016. Evolutionary polynomial
620   regression–based statistical determination of the shear capacity equation for
621   reinforced concrete beams without stirrups. Journal of Computing in Civil
622   Engineering, 30(1), p.04014111.

623   Giustolisi, O. and Savic, D.A., 2006. A symbolic data-driven technique based on
624   evolutionary polynomial regression. Journal of Hydroinformatics, 8(3), pp.207-222.

625   Giustolisi, O. and Savic, D.A., 2009. Advances in data-driven analyses and
626   modelling using EPR-MOGA. Journal of Hydroinformatics, 11(3-4), pp.225-236.

627   Goh, A.T.C., 1995. Empirical design in geotechnics using neural networks.
628   Géotechnique, 45(4), pp.709-714.

629   Harandizadeh, H., Armaghani, D.J. and Khari, M., 2019. A new development of
630   ANFIS–GMDH optimized by PSO to predict pile bearing capacity based on
631   experimental datasets. Engineering with Computers, pp.1-16.

632   Harandizadeh, H., Toufigh, M.M. and Toufigh, V., 2018a. Application of improved
633   ANFIS approaches to estimate bearing capacity of piles. Soft Computing, DOI:
634   https://doi.org/10.1007/s00500-018-3517-y.

635   Harandizadeh, H., Toufigh, M.M. and Toufigh, V., 2018b. Different neural networks
636   and modal tree method for predicting ultimate bearing capacity of piles. International
637   Journal of Optimization in Civil Engineering, 8(2), pp.311-328.

638   Huang, C.F., Li, Q., Wu, S.C., Liu, Y. and Li, J.Y., 2019. Assessment of empirical
639   equations of the compression index of muddy clay: sensitivity to geographic locality.
640   Arabian Journal of Geosciences, 12(4), p.122.

641 International Organization for Standardization (ISO), 2016. Petroleum and natural

642 gas industries-specific requirements for offshore structures. Part 4: geotechnical and

643 foundation design considerations. ISO 19901-4:2016, Geneva, Switzerland.

644 Ismail, A. and Jeng, D.S., 2011. Modelling load–settlement behaviour of piles using

645 high-order neural network (HON-PILE model). Engineering Applications of Artificial

646 Intelligence, 24(5), pp.813-821.

647 Li, J., Wang, X., Guo, Y. and Yu, X.B., 2019. Vertical bearing capacity of the pile

648 foundation with restriction plate via centrifuge modelling. Ocean Engineering, 181,

649 pp.109-120.

650 Milad, F., Kamal, T., Nader, H. and Erman, O.E., 2015. New method for predicting the

651 ultimate bearing capacity of driven piles by using Flap number. KSCE Journal of Civil

652 Engineering, 19(3), pp.611-620.

653 Moayedi, H. and Armaghani, D.J., 2018. Optimizing an ANN model with ICA for

654 estimating bearing capacity of driven pile in cohesionless soil. Engineering with

655 Computers, 34(2), pp.347-356.

656 Moayedi, H. and Hayati, S., 2018a. Applicability of a CPT-based neural network

657 solution in predicting load-settlement responses of bored pile. International Journal

658 of Geomechanics, 18(6), p.06018009.

659 Moayedi, H. and Hayati, S., 2018b. Artificial intelligence design charts for predicting

660 friction capacity of driven pile in clay. Neural Computing and Applications, DOI:

661 https://doi.org/10.1007/s00521-018-3555-5.

662 Mohammadzadeh D.S., Kazemi S.F., Mosavi A., Nasseralshariati E. and Joseph H.

663 M. Tah. J.H.M., 2019. Prediction of Compression Index of Fine-Grained Soils Using

664 a Gene Expression Programming Model. Infrastructures, 4(2), 26.

665 Momeni, E., Nazir, R., Armaghani, D.J. and Maizir, H., 2014. Prediction of pile bearing

666 capacity using a hybrid genetic algorithm-based ANN. Measurement, 57, pp.122-131.

667   Momeni, E., Nazir, R., Armaghani, D.J. and Maizir, H., 2015. Application of artificial
668   neural network for predicting shaft and tip resistances of concrete piles. Earth
669   Sciences Research Journal, 19(1), pp.85-93.

670   Nassr, A., Esmaeili-Falak, M., Katebi, H. and Javadi, A., 2018b. A new approach to
671   modeling the behavior of frozen soils. Engineering Geology, 246, pp.82-90.

672   Nassr, A., Javadi, A. and Faramarzi, A., 2018a. Developing constitutive models from
673   EPR-based self-learning finite element analysis. International Journal for Numerical
674   and Analytical Methods in Geomechanics, 42(3), pp.401-417.

675   Nejad, F.P. and Jaksa, M.B., 2017. Load-settlement behavior modeling of single
676   piles using artificial neural networks and CPT data. Computers and Geotechnics, 89,
677   pp.9-21.

678   Onyejekwe, S., Kang, X. and Ge, L., 2015. Assessment of empirical equations for the
679   compression index of fine-grained soils in Missouri. Bulletin of Engineering Geology
680   and the Environment, 74(3), pp.705-716.

681   Ozer, M., Isik, N.S. and Orhan, M., 2008. Statistical and neural network assessment
682   of the compression index of clay-bearing soils. Bulletin of Engineering Geology and
683   the Environment, 67(4), pp.537-545.

684   Prayogo, D. and Susanto, Y.T.T., 2018. Optimizing the prediction accuracy of friction
685   capacity of driven piles in cohesive soil using a novel self-tuning least squares support
686   vector machine. Advances in Civil Engineering, 2018.

687   Samui, P., 2008. Prediction of friction capacity of driven piles in clay using the support
688   vector machine. Canadian Geotechnical Journal, 45(2), pp.288-295.

689   Samui, P., 2011. Prediction of pile bearing capacity using support vector machine.
690   International Journal of Geotechnical Engineering, 5(1), pp.95-102.

691   Samui, P., 2019. Determination of Friction Capacity of Driven Pile in Clay Using
692   Gaussian Process Regression (GPR), and Minimax Probability Machine Regression
693   (MPMR). Geotechnical and Geological Engineering, pp.1-5.

694 Shahin, M.A., 2010. Intelligent computing for modeling axial capacity of pile

695 foundations. Canadian Geotechnical Journal, 47(2), pp.230-243.

696 Shahin, M.A., 2014a. Load–settlement modeling of axially loaded drilled shafts using

697 CPT-based recurrent neural networks. International Journal of Geomechanics, 14(6),

698 p.06014012.

699 Shahin, M.A., 2014b. Load–settlement modeling of axially loaded steel driven piles

700 using CPT-based recurrent neural networks. Soils and Foundations, 54(3), pp.515-

701 522.

702 Shahin, M.A., 2016. State-of-the-art review of some artificial intelligence applications

703 in pile foundations. Geoscience Frontiers, 7(1), pp.33-44.

704 Shaik, S., Krishna, K.S.R., Abbas, M., Ahmed, M. and Mavaluru, D., 2018. Applying

705 several soft computing techniques for prediction of bearing capacity of driven piles.

706 Engineering with Computers, DOI: https://doi.org/10.1007/s00366-018-0674-7.

707 Singh, G. and Walia, B.S., 2017. Performance evaluation of nature-inspired

708 algorithms for the design of bored pile foundation by artificial neural networks. Neural

709 Computing and Applications, 28(1), pp.289-298.

710 Sladen, J.A., 1992. The adhesion factor: applications and limitations. Canadian

711 Geotechnical Journal, 29(2), pp.322-326.

712 Sladen, J.A., 1992. The adhesion factor: applications and limitations. Canadian

713 Geotechnical Journal, 29(2), pp.322-326.

714 Stas, C.V. and Kulhawy, F.H., 1984. Critical evaluation of design methods for

715 foundations under axial uplift and compression loading. Report for EPRI, No.

716 EL3771, Cornell University.

717 Suman, S., Das, S.K. and Mohanty, R., 2016. Prediction of friction capacity of driven

718 piles in clay using artificial intelligence techniques. International Journal of

719 Geotechnical Engineering, 10(5), pp.469-475.

720   Terzaghi, K., Peck, R.B. and Mesri, G., 1996. Soil mechanics in Engineering

721   Practice. John Wiley & Sons.

722   Tinoco, J., Alberto, A., da Venda, P., Correia, A.G. and Lemos, L., 2019. A novel

723   approach based on soft computing techniques for unconfined compression strength

724   prediction of soil cement mixtures. Neural Computing and Applications,

725   https://doi.org/10.1007/s00521-019-04399-z

726   Vijayvergiya, V. A. and Focht, J. A., Jr., 1972. A new way to predict capacity of piles

727   in clays. Proceedings of the 4th Offshore Technology Conference, Houston 2, 865-

728   874.